JOURNAL OF COMPUTATIONAL PHYSICS 53, 331–345 (1984)

Fast Scheme for Photon-Maxwellian Electron Cross Sections

B. R. WIENKE AND B. L. LATHROP

Computing Division, Los Alamos National Laboratory, Los Alamos, New Mexico 87545

Received February 8, 1983

A fast and accurate method for computing temperature-corrected photon-Maxwellian electron cross sections with distribution averaged electron energies and scattering angles in presented. Use is made of the covariant (frame indepedent) picture of scattering for relativistic electrons. The scheme is motivated and detailed, predictions are obtained and compared with exact values and appropriate limiting forms which retain the Thomson and Klein–Nishina cross section structure are also recovered. The method is amenable to further pointwise (Monte Carlo) or multigroup (S_n) cross section processing. A two parameter fit to the relativistic cross sections is also described that resembles the Klein–Nishina formula in structure and can be used to generate temperature corrections within existning static electron algorithms.

1. INTRODUCTION

Photon downscatter (Compton) and upscatter (inverse Compton) from Maxwellian electrons is an important feature of radiative transport calculations in both Monte Carlo and discrete ordinates applications. The general description of photon-Maxwellian electron scattering is numerically complex and computationally time consuming. It is our purpose to describe a fast and accurate method for generating effective radiative transfer kernels for relativistic Maxwellian electrons and to compare predictions with exact results. Appropriate limiting forms are also recovered. Use is made of the covariant (frame independent) picture of scattering [1] and the distribution averaged electron energies and scattering angles [2]. The scheme is motivated and detailed, predictions are compared and limiting forms which recover the well-known Thomson and Klein–Nishina [3] formulas are also exhibited with temperature corrections. This approach serves as a useful alternative to time consuming numerical integration of the 5-dimensional Lorentz kernel [4, 5] and as an exact alternative to low-order expansions [5–7] in temperature or incidient photon energy. The equations are directly amenable to pointwise or multigroup implementation in Monte Carlo or S_n transport codes [8–10]. Much of the following analysis has been implemented and tailored for use in Los Alamos based transport modules. Stimulated emission, of course, is ignored in the analysis.

We considered three related segments in the following scheme. The first is a lowest order, zero electron momentum approximation which imparts small temperature

0021-9991/84 $3.00

corrections to the usual, stationary Klein–Nishina cross section. For incident photon energy greater than the background electron temperature, it is simple and accurate. The second approach extends the low energy approximation by assuming that the distributionally averaged photon scattering angle is zero but relaxes the requirement of zero electron momentum. The second approach works very well for incident photon energy less than, or close to, the background electron temperature. Finally, in an effort to simplify matters further, a two parameter fit to the differential cross section is proposed and described. The fit equation resembles the well-known stationary electron expression (with only one angular dependence) and is useful in computational algorithms that already employ, or sample, the Klein–Nishina result (such as those used in Monte Carlo photonics). The two parameter fitted equations recover exact total cross sections to three significant figures over the full energy and temperature spectrum. We refer to these segments as the low energy, isotropic and fitted approximations, and have found all three useful in various radiative transport applications.

Natural units ($\hbar = c = k = 1$) are employed both as a convenience and convention, that is, with $\hbar$ Planck's constant, c the speed of light, and k Boltzmann's constant. To convert the macroscopic cross sections defined herein to inverse mean free paths for radiation transport, one only needs to multiply all expressions by the electron number density.

2. Transfer Kernels and Kinematics

Denoting incoming photon and electron energies by v' and ε' and outgoing photon and electron energies by v and ε, with corresponding electron momenta p', p, the relativistic energy balance equation for scattering can be expressed as [1, 11, 12],

$$\varepsilon' v' - p' v' \cos\alpha' = v v'(1 - \cos\Theta) + \varepsilon' v - p' v \cos\alpha \tag{1}$$

with,

$$\cos\alpha = \cos\alpha' \cos\Theta + \sin\alpha' \sin\Theta \cos\phi, \tag{2}$$

where α' and α are the angles between incident electron and incident and final photons, Θ is the angle between incident and final photons, and ϕ is the azimuthal orientation of the scattered photon. Alternatively, Eq. (1) can also be written as,

$$\varepsilon^2 = \varepsilon'^2 + v^2 + v'^2 + 2p'v' \cos\alpha' - 2p'v \cos\alpha - 2vv' \cos\Theta. \tag{3}$$

Equations (1) and (3) accommodate upscatter and downscatter.

The Lorentz invariant kernel for scattering of an incident photon of energy v' from a background Maxwellian electron distribution $f(\bar{p}')$ takes the form [11, 12]

$$\begin{aligned}\frac{\partial^2\sigma}{\partial\Omega\,\partial v} = \frac{r_0^2}{2}\int d^3p' f(\mathbf{p}') \left(\frac{m^2 v}{\varepsilon' v'}\right) \\ \times \delta[\varepsilon' v' - p' v' \cos\alpha' - v v'(1 - \cos\Theta) - \varepsilon' v + p' v \cos\alpha]\, K\end{aligned} \tag{4}$$

with,

$$K = \frac{m^4(1-\cos\Theta)^2}{(\varepsilon' - p'\cos\alpha')^2\,(\varepsilon' - p'\cos\alpha)^2} - \frac{2m^2(1-\cos\Theta)}{(\varepsilon' - p'\cos\alpha')(\varepsilon' - p'\cos\alpha)} + \frac{v'(\varepsilon' - p'\cos\alpha')}{v(\varepsilon' - p'\cos\alpha)} + \frac{v(\varepsilon' - p'\cos\alpha)}{v'(\varepsilon' - p'\cos\alpha')}. \tag{5}$$

Equation (4) is a Lorentz scalar in all coordinate frames. In the rest frame of the electron or for stationary electrons in the laboratory ($p' = 0$, $\varepsilon' = m$), Eq. (4) reduces to the classical Klein–Nishina law. In the above, r_0 is the classical electron radius and m is the electron rest mass. The relativistic momentum distribution is taken to be the Maxwellian expression,

$$f(\mathbf{p}') = (4\pi\gamma)^{-1}\exp[-(p'^2 + m^2)^{1/2}/T] \tag{6}$$

with,

$$\gamma = m^2 T K_2(m/T) \tag{7}$$

for K_2 the modified Bessel function and T the temperature.

Pomraning [13] has detailed a velocity representation of the effective scattering kernel which we have shown [14] to be equivalent to Eq. (4), we do not recount the procedure here. Both representations are relativistic but Eq. (4) is more convenient for our purposes. Note also that apart from the kinematical factors $(\varepsilon' - p'\cos\alpha')$ and $(\varepsilon' - p'\cos\alpha)$, the scattering kernel equation (5) has been cast in the Klein–Nishina form with one exception. The kinematical equation (1) permits both upscatter and downscatter whereas the usual Compton law only allows downscatter.

The integration over $d^3p'\,d\Omega\,dv$ in Eq. 4 is formidable. The δ-function permits one integration over dv trivially. At best, one is faced with a 4-dimensional integration which is time consuming even on supercomputers such as the Cray–1. Typical Cray–1 run times for evaluation of the cross section σ using Eq. (4), directly average 1–2 min using nested adaptive quadrature routines. In production transport codes, one is not allowed the luxury of minutes for pointwise cross section processing and obviously a fast and accurate scheme is necessary. In the following we detail a scheme which permits efficient evaluation of Eq. (4) and uses the distribution weighted (averaged) electron momenta and scattering angles to replace the tedious integration over d^3p'. Operationally, one replaces the Maxwellian distribution with

$$f(\mathbf{p}') = \frac{\delta(p' - \langle p'\rangle)\,\delta(\cos\alpha' - \langle\cos\alpha'\rangle)}{2\pi p'^2} \tag{8}$$

for $\langle p'\rangle$ and $\langle\cos\alpha'\rangle$ the appropriately determined mean electron momentum and scattering angle. Before considering the scheme, we turn to integration of the energy δ-function and determination of various moments of the Maxwellian distribution.

Invoking the operational definition for arbitrary function g,

$$\delta(g) = \left| \frac{\partial g}{\partial v} \right|_{v_0}^{-1} \delta(v - v_0) \tag{9}$$

with $g(v_0) = 0$ and,

$$\left| \frac{\partial g}{\partial v} \right|_{v_0}^{-1} = \frac{1}{v'(1 - \cos\Theta) + \varepsilon' - p' \cos\alpha} = \frac{v}{\varepsilon' v' - p' v' \cos\alpha'}, \tag{10}$$

we recast Eq. (4) in the convenient form after integrating over dv,

$$\frac{\partial \sigma}{\partial \Omega} = \frac{r_0^2}{2} \int d^3p' f(\mathbf{p}') \frac{m^2}{\varepsilon'(\varepsilon' - p' \cos\alpha')} \left(\frac{v}{v'}\right)^2 K. \tag{11}$$

It will also be advantageous to introduce the dimensionless parameters κ, κ_1, and κ_2,

$$\begin{aligned} \kappa m &= \varepsilon', \\ \kappa_1 m &= \varepsilon' - p' \cos\alpha' = \kappa m - (\kappa^2 - 1)^{1/2} m \cos\alpha', \\ \kappa_2 m &= \varepsilon' - p' \cos\alpha = \kappa m - (\kappa^2 - 1)^{1/2} m \cos\alpha, \end{aligned} \tag{12}$$

so that Eq. (1) takes the simple form,

$$\kappa_1 m v' = v v'(1 - \cos\Theta) + \kappa_2 m v, \tag{13}$$

in analogy with the Compton expression. For $\kappa_1 > \kappa_2$, upscatter is kinematically possible while for $\kappa_1 \leqslant \kappa_2$ only downscatter results. For $\kappa_1 = \kappa_2 = \kappa = 1$ ($\varepsilon' = m$, $p' = 0$), the classical Compton law is recovered.

3. Relativistic Maxwellian Electron Distribution

The previously defined relativistic Maxwellian electron distribution function $f(\mathbf{p}')$, was written,

$$f(\mathbf{p}') = (4\pi\gamma)^{-1} \exp[-(p'^2 + m^2)^{1/2}/T] \tag{14}$$

with T the absolute temperature and γ the normalization constant,

$$\gamma = \int_0^\infty \exp[-(p'^2 + m^2)^{1/2}/T]\, p'^2\, dp'. \tag{15}$$

Defining the nth normalized moment of f as

$$\langle p'^n \rangle = \gamma^{-1} \int_0^\infty \exp[-(p'^2 + m^2)^{1/2}/T]\, p'^{n+2}\, dp', \tag{16}$$

we have shown [2] by transforming to energy space,

$$\begin{aligned}
\gamma &= m^2 T K_2(m/T), \\
\langle p' \rangle &= m \left(\frac{8T}{\pi m}\right)^{1/2} \frac{K_{5/2}(m/T)}{K_2(m/T)}, \\
\langle p'^2 \rangle &= m^2 \left(\frac{3T}{m}\right) \frac{K_3(m/T)}{K_2(m/T)}, \\
\langle p'^n \rangle &= m\gamma^{-1} \left(\Gamma\left(\frac{n+3}{2}\right) \Big/ \Gamma(1/2)\right) (2mT)^{(n+2)/2} K_{(n+4)/2}(m/T),
\end{aligned} \tag{17}$$

with K the modified Bessel functions and Γ the Euler functions.

For low temperazture $m/T \gg 1$, it follows [15] that

$$\begin{aligned}
\gamma &\sim m^2 T \left(\frac{\pi T}{2m}\right)^{1/2} \exp(-m/T) \left(1 + \frac{15T}{8m} \cdots\right), \\
\langle p' \rangle &\sim m \left(\frac{8T}{\pi m}\right)^{1/2} \left(1 + \frac{9T}{8m} \cdots\right), \\
\langle p'^2 \rangle &\sim m^2 \left(\frac{3T}{m}\right) \left(1 + \frac{20T}{8m} \cdots\right),
\end{aligned} \tag{18}$$

which are precisely the classical, nonrelativistic values. Furthermore, for $p'/m \ll 1$,

$$(p'^2 + m^2)^{1/2} \sim m \left(1 + \frac{p'^2}{2m^2} \cdots\right) \tag{19}$$

so that we recover the nonrelativistic law from Eqs. (14), (18), and (19),

$$f(\mathbf{p}') \sim (2\pi mT)^{-3/2} \exp(-p'^2/2mT). \tag{20}$$

Higher order terms in Eqs. (18) and (19) are the temperature and relativistic corrections.

4. Low Energy Approximation and Some Limiting Forms

Rather than perform the 3-dimensional integration over $f(\mathbf{p}')$, we replace the kernel with an appropriately averaged expression for $\langle p' \rangle$ and $\langle \cos \alpha' \rangle$ using Eq. (8). The energy $\langle \varepsilon' \rangle$ and momentum $\langle p' \rangle$ are easily obtained from Eqs. (17), so that Eqs. (12) are recast,

$$\kappa m = \langle \varepsilon' \rangle = [\langle p'^2 \rangle + m^2]^{1/2} = \left[\left(\frac{3T}{m}\right) \frac{K_3(m/T)}{K_2(m/T)} + 1 \right]^{1/2}. \tag{21}$$

and,

$$\kappa_1 m = \kappa m + (\kappa^2 - 1)^{1/2}\, m\langle \cos \alpha' \rangle, \qquad \kappa_2 m = \kappa m + (\kappa^2 - 1)^{1/2}\, m \cos \alpha, \quad (22)$$

with,

$$\cos \alpha = \langle \cos \alpha' \rangle \cos \Theta + \langle \sin \alpha' \rangle \sin \Theta \cos \phi. \quad (23)$$

While it is possible to obtain $\langle \varepsilon' \rangle$, $\langle p' \rangle$, and κ directly from Eq. (21), evaluation of $\langle \cos \alpha' \rangle$ is not generally possible analytically. In the following we examine the $\langle \cos \alpha' \rangle \to 0$ case and in a later section consider a bootstrap fit to $\langle \cos \alpha' \rangle$ over a range of energies and temperatures. Equation (11) thus becomes, using Eqs. (8), (21)–(23) and integrating over $d\phi'$ trivially,

$$\frac{\partial \sigma}{\partial \Omega} = \left(\frac{r_0^2}{2}\right)\left(\frac{1}{\kappa \kappa_1}\right)\left(\frac{v}{v'}\right)^2 K,$$
$$K = \frac{(1 - \cos \Theta)^2}{(\kappa_1 \kappa_2)^2} - \frac{2(1 - \cos \Theta)}{(\kappa_1 \kappa_2)} + \frac{\kappa_1 v'}{\kappa_2 v} + \frac{\kappa_2 v}{\kappa_1 v'}, \quad (24)$$

with, from Eq. (13),

$$\left(\frac{v}{v'}\right) = \frac{\kappa_1 m}{v'(1 - \cos \Theta) + \kappa_2 m}. \quad (25)$$

Experience has shown that Eqs. (21)–(25) provide a relatively simple and accurate representation for describing photon-Maxwellian electron scattering [1, 2, 10, 11]. Consider the low energy approximation and recovery of some well-known results.

In the *low energy* limit, $(\kappa^2 - 1)^{1/2} \to 0$, $\kappa = \kappa_1 = \kappa_2$, we find from Eq. (24),

$$\frac{\partial \sigma}{\partial \Omega} = \left(\frac{r_0^2}{2}\right)\left(\frac{1}{\kappa^2}\right)\left(\frac{v}{v'}\right)^2 \left[\frac{(1 - \cos \Theta)^2}{\kappa^4} - \frac{2(1 - \cos \Theta)}{\kappa^2} + \frac{v'}{v} + \frac{v}{v'}\right], \quad (26)$$

which is the temperature corrected Klein–Nishina law. The usual Klein–Nishina expression obtains for $k = 1$. For low incident photon energy, $v' \to 0$, we have from Eq. (25),

$$\lim_{v' \to 0} \left(\frac{v}{v'}\right) = \lim_{v' \to 0} \frac{\kappa m}{v'(1 - \cos \Theta) + \kappa m} = 1 \quad (27)$$

so that the temperature-corrected Thomson cross section becomes, using Eq. (26),

$$\frac{\partial \sigma}{\partial \Omega} = \left(\frac{r_0^2}{2}\right)\left(\frac{1}{\kappa^2}\right)\left[\frac{(1 - \cos \Theta)^2}{\kappa^4} - \frac{2(1 - \cos \Theta)}{\kappa^2} + 2\right] \quad (28)$$

with $\kappa = 1$ the classical result. In the high energy regime, $v' \to \infty$, only the second last term of Eq. (26) survives and we deduce the temperature modified Bjorken [17] relationship,

$$\frac{\partial\sigma}{\partial\Omega} = \left(\frac{r_0^2}{2}\right)\left(\frac{1}{\kappa^2}\right)\left(\frac{v}{v'}\right). \tag{29}$$

Comparisons of approximate *low energy* total cross sections obtained from Eq. (26) and exact predictions from Eq. (11) appear in Figs. 1 and 2. Best agreement occurs for $v' > T$ since the incident photon tends to view most of the electrons as stationary. As $v' < T$, many electrons upscatter the incident photon and the low-energy scheme falls short of predicting the total cross section. In the above and following calculations,

$$r_0^2 = 0.07938 \times 10^{-24}\ \text{cm}^2, \tag{30}$$

and photon energies and electron temperatures range,

$$\begin{aligned} &0\ \text{keV} \leqslant T \leqslant 100\ \text{keV}, \\ &0\ \text{keV} \leqslant v' \leqslant 1\ \text{MeV}. \end{aligned} \tag{31}$$

As T becomes small, both sets of cross sections give the Klein–Nishina limit as required ($\alpha = v'/m$),

$$\sigma = 2\pi r_0^2 \left\{\frac{2}{\alpha^2} + \left[\frac{1}{2\alpha} - \frac{(1+\alpha)}{\alpha^3}\right]\ln(1+2\alpha) + \frac{(1+\alpha)}{(1+2\alpha)^2}\right\}. \tag{32}$$

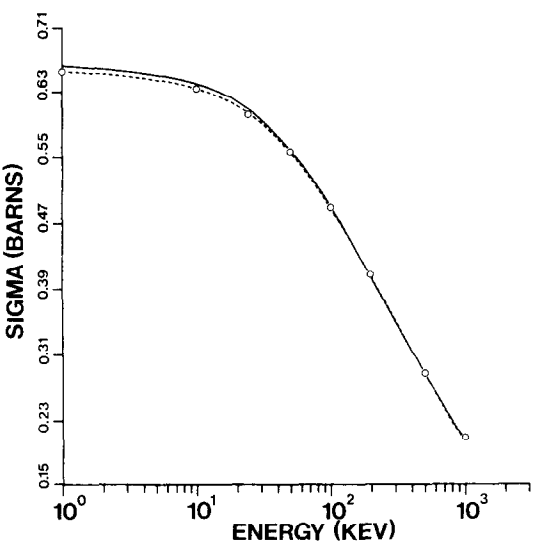

FIG. 1. Low energy total cross section ($T = 1$ keV). Solid line, exact; dotted line, low energy approximation.

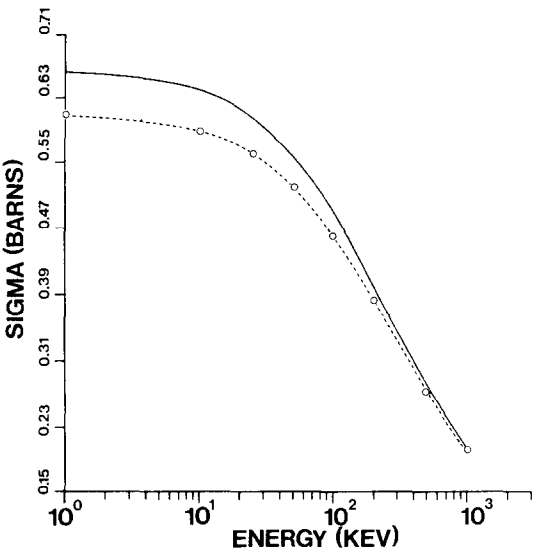

FIG. 2. Low energy total cross section ($T = 10$ keV). Solid line, exact; dotted line, low energy approximation.

As both v', T approach zero, both sets approach the Thomson limit,

$$\sigma = 8\pi r_0^2/3. \tag{33}$$

5. Isotropic Scattering Approximation

The *low energy* ($p' \to 0$) cross sections exhibited in Figs. 1 and 2 are not adequate as $v' < T$, a situation in which a significant portion of the electrons upscatter the incident photon. The $p' \to 0$ limit drops all terms involving $\langle \cos \alpha' \rangle$ and $\cos \alpha$ out of Eqs. (22) and (23), so that resulting expressions are really temperature corrected, static (Klein–Nishina-like) predictions, good for $v' > T$. The next higher order scheme is probably obvious and is based on a simple physical argument.

Except for very large differences between v' and T, one might reasonably argue that the photon views the electron distribution isotropically as far as an average scattering angle is concerned. Therefore, in the *isotropic* approximation ($p' \neq 0$), we take,

$$\langle \cos \alpha' \rangle = 0, \tag{34}$$

as our starting point, so that Eqs. (22) and (23) are recast,

$$\begin{aligned} \kappa_1 m &= \kappa m, \\ \kappa_2 m &= \kappa m - (\kappa^2 - 1)^{1/2} m \cos \alpha, \end{aligned} \tag{35}$$

and

$$\cos\alpha = \sin\Theta\cos\phi. \tag{36}$$

The balance equation, Eq. (13), now admits upscatter and downscatter as $0 < \phi \leqslant 2\pi$ while the differential cross section depends explicitly on both Θ and ϕ in a more complex manner. The *isotropic* approximation, $\langle\cos\alpha'\rangle \to 0$, is excellent as can be seen in Figs. 3 and 4 which plot exact (solid lines) cross sections from Eq. (11) against Eq. (24) using Eqs. (35) and (36) (dotted lines). Agreement at the 2–3% level is seen over depicted ranges. In analogy with Eq. (26), we write in the *isotropic* limit,

$$\frac{\partial\sigma}{\partial\Omega} = \left(\frac{r_0^2}{2}\right)\left(\frac{1}{\kappa^2}\right)\left(\frac{\nu}{\nu'}\right)^2\left[\frac{(1-\cos\Theta)}{(\kappa\kappa_2)^2} - \frac{2(1-\cos\Theta)}{(\kappa\kappa_2)} + \frac{\kappa\nu'}{\kappa_2\nu} + \frac{\kappa_2\nu}{\kappa\nu'}\right], \tag{37}$$

with,

$$\left(\frac{\nu}{\nu'}\right) = \frac{\kappa m}{\nu'(1-\cos\Theta) + \kappa m - (\kappa^2-1)^{1/2}\, m\sin\Theta\cos\phi}. \tag{38}$$

To scope agreement in differential parameters, Figs. 5–8 plot $\partial\sigma/\partial\Theta$ using Eqs. (11) and (37) for various incident photon energies and temperatures. Clearly, best agreement in the differential cross sections, as with the total cross sections, occurs for $\nu' > T$. Agreement overall is still good.

The added price for this agreement, however, is the introduction of an azimuthal dependence in the differential cross section. Next we will examine a representation for

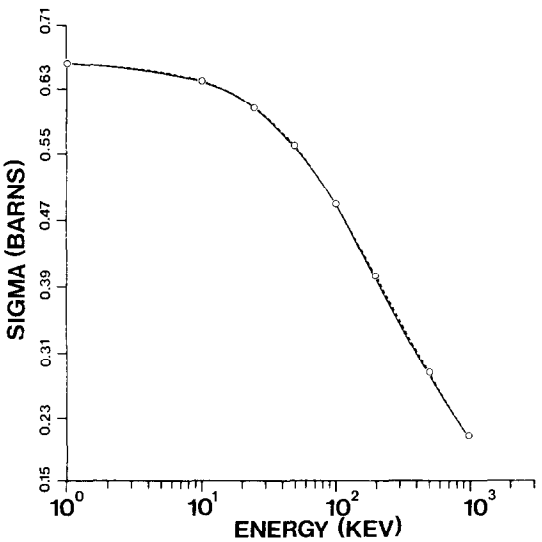

FIG. 3. Isotropic total cross section ($T = 10$ keV). Solid line, exact; dotted line, isotropic approximation.

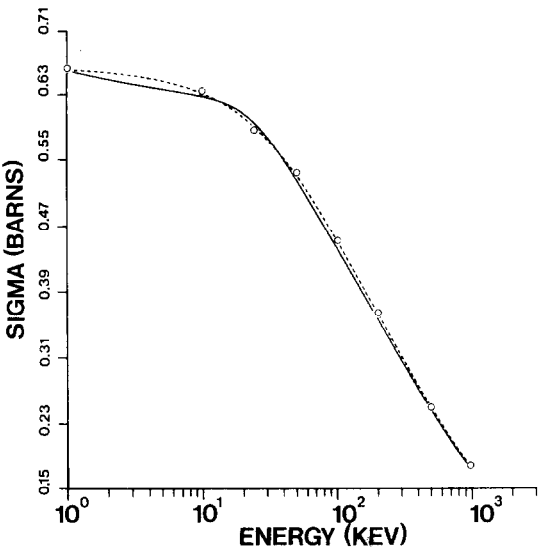

FIG. 4. Isotropic total cross section ($T = 100$ keV). Solid line, dotted line, isotropic approximation.

which all angular dependences, except the usual cos Θ terms, have been averaged out of the explicit expressions for κ_1 and κ_2. Such an approach amounts to an energy parameter fit to the differential cross section, Eq. (24), using κ_1 and κ_2 that easily and directly replaces code algorithms that employ the Klein–Nishina expression ($T = 0$).

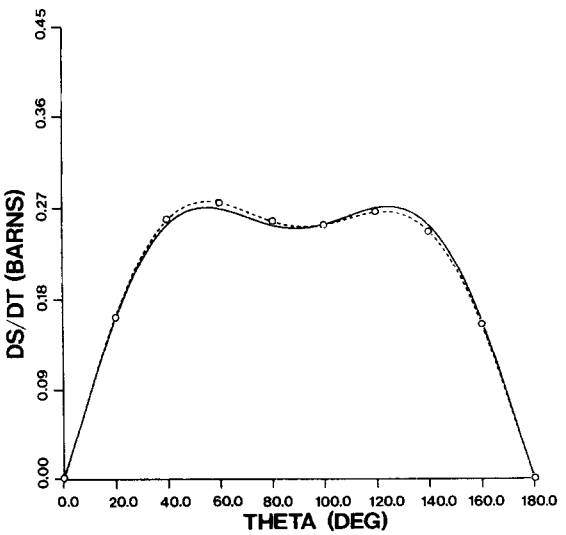

FIG. 5. Isotropic differential cross section ($T = 1$ keV, photon energy = 1 keV). Solid line, exact; dotted line, isotropic approximation.

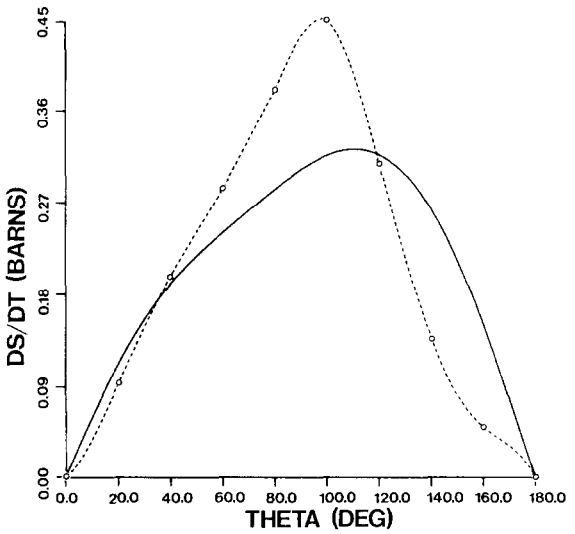

FIG. 6. Isotropic differential cross section ($T = 100$ keV, photon energy = 1 keV). Solid line, exact; dotted line, isotropic approximation.

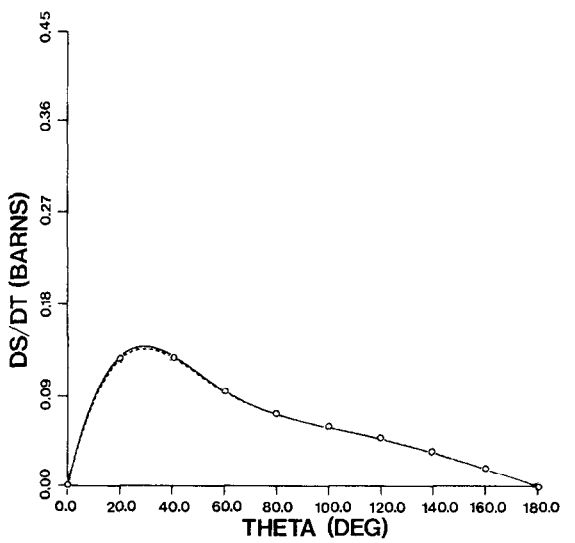

FIG. 7. Isotropic differential cross section ($T = 1$ keV, photon energy = 1000 keV). Solid line, exact; dotted line, isotropic approximation.

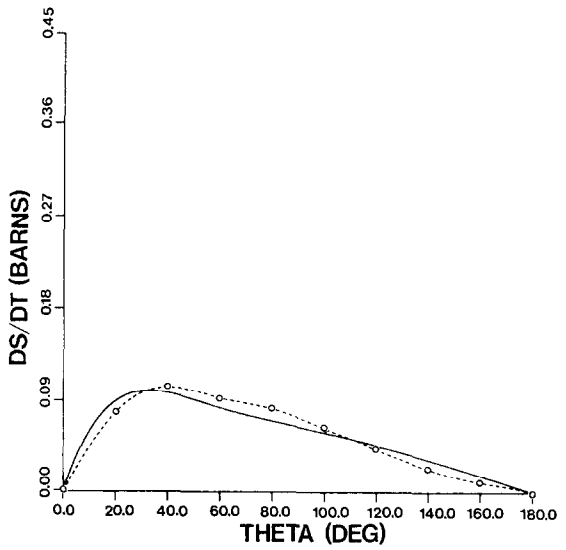

FIG. 8. Isotropic differential cross section ($T = 100$ keV, photon energy = 1000 keV). Solid line, exact; dotted line, isotropic approximation.

6. FITTED APPROXIMATION

Rather than performing the time consuming numerical integrations over $\cos\alpha'$ and ϕ in Eq. (5) or over ϕ in Eq. (24) with $\langle\cos\alpha'\rangle = 0$, it is tempting and advantageous to treat κ_1 and κ_2 as a set of fitting parameters to either differential, or total, cross sections. All bothersome intermediate angular integrations are effectively averaged out of the calculation and eliminated. The resulting kernel is Klein-Nishina-like and written, in the *fitted* approximation, as,

$$\frac{\partial\sigma}{\partial(\cos\Theta)} = \pi r_0^2 \left(\frac{1}{\kappa\langle\kappa_1\rangle}\right)\left(\frac{v}{v'}\right)^2 K, \tag{39}$$

with κ still given by Eq. (21) and,

$$\begin{aligned} K &= \frac{(1-\cos\Theta)^2}{(\langle\kappa_1\rangle\langle\kappa_2\rangle)^2} - \frac{2(1-\cos\Theta)}{(\langle\kappa_1\rangle\langle\kappa_2\rangle)} + \frac{v'}{v} + \frac{v}{v'}, \\ \left(\frac{v}{v'}\right) &= \frac{\langle\kappa_1\rangle m}{v'(1-\cos\Theta) + \langle\kappa_2\rangle m}, \end{aligned} \tag{40}$$

for $\langle\kappa_1\rangle$ and $\langle\kappa_2\rangle$ arbitrary at this point. Equations (39) and (40) with $\kappa = \langle\kappa_1\rangle = \langle\kappa_2\rangle = 1$ are already employed in many applications codes. Tabulation of temperature corrected values of $\langle\kappa_1\rangle$ and $\langle\kappa_2\rangle$ would obviously permit easy operational extension

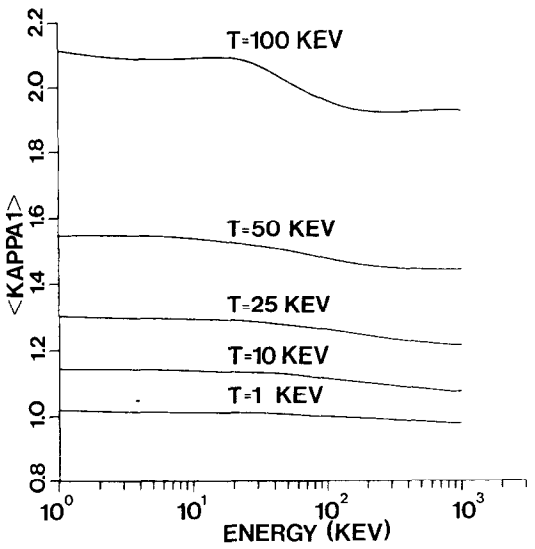

FIG. 9. Total cross section fitting parameter for various temperatures.

of the static algorithms to include scattering from a Maxwellian electron background at little or no added computing price. As before, $\langle \kappa_1 \rangle > \langle \kappa_2 \rangle$ underscores photon upscatter in energy while $\langle \kappa_1 \rangle \leqslant \langle \kappa_2 \rangle$ tags downscatter. Any fit to the exact cross sections over photon energies and electron temperatures should reasonably reflect those kinematics on the average. Additionally, as the temperature approaches zero, one expects $\langle \kappa_1 \rangle \to \langle \kappa_2 \rangle \to 1$.

Integrating Eq. (39) exactly yields a functional form with which we fit the exact cross sections over the ranges indicated in Eqs. (31) subject to the foregoing constraints and the additional simplification,

$$\langle \kappa_2 \rangle = \kappa, \tag{41}$$

suggested by Eq. (22) in averaging cos α freely over ϕ in the $\langle \cos \alpha' \rangle \to 0$ limit. Alternatively, one might view Eq. (41) as a convenient starting point. Results of this parametrization appear in Fig. 9 which plots $\langle \kappa_1 \rangle$ versus v' for $T = 1$, 10, 25, 50, and 100 keV, or, equivalently from Eq. 21, for $\kappa = 1.002$, 1.030, 1.079, 1.170, 1.381. This fit reproduces the total cross sections to 3 significant figures. Correspondingly *fitted* differential cross predictions are roughly the same as those depicted in Figs. 5–8 in Section 5, though not quite as good for increasing temperature. Note in Fig. 9 that as the background electron temperatures increase relative to the incident photon energy, $\langle \kappa_1 \rangle$ increases, and that as temperatures get small, $\langle \kappa_1 \rangle \to 1$, consistent with the scattering physics.

The *fitted* Eqs. (39) and (40) from Fig. 9 are useful temperature-corrected replacements for stationary electron algorithms when the *low energy* approach is not

accurate enough and the *isotropic* scheme, with extra integration over ϕ, is costlier than desired.

7. Conclusions

We have examined a fast and accurate scheme for generating photon-Maxwellian electron cross sections in both low energy, $p' \to 0$, and isotropic, $\langle \cos \alpha' \rangle \to 0$, limits. Best results obtain for $v' > T$ in both cases, but the isotropic approximation yields excellent results over the full range of investigation, $0 \leqslant v' \leqslant 1$ MeV, $0 \leqslant T \leqslant 100$ keV. The forms of the depicted differential and total cross sections are suitable for pointwise implementation in Monte Carlo transport codes or further multigroup [18] processing in S_n transport codes. Well-known limiting forms have also been recovered from the scheme. Results of the study indicate that the isotropic approximation is accurate at the $3n\%$ level for $T/v' \leqslant 10^n$ as far as total cross section predictions. Differential cross section predictions scale in roughly similar proportions. Using the isotropic approximation as a starting point, the results suggest the validity of a two parameter fit, employing κ_1 and κ_2, over appropriate temperature and photon energy ranges. A relatively simple parametrization of κ_1 and κ_2 as a function of v' and T, with all intermediate angular dependences eliminated, was obtained in the fitted approximation. Resulting differential cross sections only depend on $\cos \Theta$, in analogy with the usual Klein–Nishina relationship.

As a final remark, we mention that a number of production codes [19] keyed to Eqs. (11), (24), and (37) have been constructed and are available to interested users on request.

Acknowledgments

We thank J. Devaney (LANL) and G. Pomraning (UCLA) for applications testing and some technical discussions and the LANL Monte Carlo Group (X–6) for providing further impetus to the study.

References

1. B. R. Wienke, *J. Quant. Spectrosc. Radiat. Transfer* **15** (1975), 151.
2. B. R. Wienke, *Amer. J. Phys.* **43** (1975), 317
3. O. Klein and Y. Nishina, *Z. Physik* **52** (1929), 853.
4. J. B. Webster III, B. G. Stephen, and C. J. Bridgman, *J. Comput. Phys.* **14** (1974), 29.
5. G. C. Pomraning, *J. Quant. Spectrosc. Radiat. Transfer* **12** (1972), 1047.
6. P. A. M. Dirac, *Mon. Not Roy. Astron. Soc.* **85** (1925), 825.
7. F. N. Edwards, Jr., *Astrophys. J.* **117** (1953), 298.
8. Los Alamos Monte Carlo Group, "MCNP: General Purpose Monte Carlo Code for Neutron and Photon Transport," Version 2B, Los Alamos National Laboratory Code Manual, April 1982.
9. T. R. Hill, "ONETRAN: Discrete Ordinates Finite Element Code for Solution of the One-Dimensional Multigroup Transport Equations," Los Alamos Scientific Laboratory Report, No. LA–5990–MS, June 1975.

10. B. R. WIENKE, *Nucl. Sci. Eng.* **81** (1982), 302.
11. B. R. WIENKE, *J. Quant. Spectrosc. Radiat. Transfer* **19** (1978), 163.
12. R. P. FEYNMAN, *Phys. Rev.* **76** (1949), 769.
13. G. C. POMRANING, *Prog. High. Temp. Phys. Chem.* **4** (1970), 1.
14. B. R. WIENKE, *Nucl. Sci. Eng.* **60** (1976), 101.
15. M. ABRAMOWITZ AND I. STEGUN, "Handbook of Mathematical Functions," Dover, New York, 1965.
16. J. J. THOMSON, *Philos. Mag.* **13** (1907), 561.
17. J. D. BJORKEN AND S. D. DRELL, "Relativistic Quantum Mechanics," Vol. I, McGraw–Hill, New York, 1964.
18. K. D. LATHROP, "GAMLEG: Fortran Code to Produce Multigroup, Cross Sections for Photon Transport Calculations," Los Alamos Scientific Laboratory Report, No. LA–3267, April 1965.
19. B. R. WIENKE AND B. L. LATHROP, "MAXWEL: Exact Photon Cross Section Processor for Relativistic Maxwellian Electrons," Los Alamos National Laboratory Report, LA–UR 83-2227, (July, 1983); to be published in *Computer Phys. Comm.*